Araştırma Makalesi / Research Article

Computational Assessment of Zeolitic-Imidazolate Frameworks (ZIFs) for Adsorption and Diffusion Based Separation of Noble Gas Mixtures

Yeliz GÜRDAL DURĞUN*

Adana Alparslan Türkeş Bilim ve Teknoloji Üniversitesi, Biyomühendislik Bölümü, Adana, Türkiye
(ORCID: 0000-0002-6245-891X)

Abstract

Zeolite imidazolate frameworks (ZIFs) possess exceptional chemical and thermal stabilities together with tunable pore sizes, high porosities, and large surface areas which opens new and exciting application areas of ZIFs, such as gas separation and purification. Although, there have been significant number of studies investigating syngas separation performances of ZIFs, currently very little is know about their noble gas separation performances. We, therefore, computationally investigate adsorption and membrane oriented Xe/Kr and Xe/Ar separation performances of ZIF-6, ZIF-60, ZIF-65, and ZIF-79. Single component and mixture gas uptakes, Xe adsorption selectivities, gas permeabilities, and Xe permeation selectivities are predicted for all ZIFs under consideration. Our results suggest that while ZIF-79 is ideal for adsorption-based Xe separation, ZIF-60 can be considered as a promising candidate for membrane oriented separation of Xe.

Keywords: GCMC, classical MD, adsorption, diffusion

Zeolitik-İmidazolat İskelet Yapılarının Adsorpsiyon ve Difüzyon-bazlı Soy-gaz Karışımı Ayırma Potansiyellerinin Hesapsal Yöntemlerle İncelenmesi

Öz

Zeolitik-imidazolat iskelet yapılarının (ZIF), yüksek kimyasal ve termal stabiliteye sahip olmalarının yanısıra ayarlanabilir gözenek boyutları, yüksek gözeneklilikleri ve geniş yüzey alanına sahip olmaları; ZIF'ler için gaz ayırma ve saflaştırma gibi yeni ve ilgi çekici bir uygulama alanı oluşturmuştur. ZIF'lerin sentez gazları saflaştırma performanslarını araştıran çok sayıda çalışma olmasına rağmen, soy-gaz ayırma performansları hakkında çok az bilgi birikimi mevcuttur. Bu nedenle, çalışmamızda ZIF-6, ZIF-60, ZIF-65 ve ZIF-79'un adsorpsiyon ve difüzyona dayalı Xe/Kr ve Xe/Ar ayırma performanslarının hesaplamalı yöntemlerle araştırılması amaçlanmıştır. Tek bileşenli ve karışım gaz adsorpsiyonları, Xe adsorpsiyon seçiciliği, gaz geçirgenliği ve Xe geçirgenlik seçiciliği araştırdığımız ZIF'ler için tahmin edilmiştir. Sonuçlarımız, ZIF-79'un adsorpsiyona dayalı Xe ayrımı için ideal olmasına rağmen, ZIF-60'ın Xe'nin membran bazlı ayırımı için umut vaadeden bir aday olarak kabul edilebileceğini göstermektedir.

Anahtar Kelimeler: GCMC, klasik moleküler dinamik, adsorpsiyon, difüzyon

1. Introduction

There has been a significant development in the adsorption, diffusion, and separation of gas mixtures using nanoporous materials. Having pioneered the synthesis of new materials, Park and Yaghi et. al [1] introduced a higly porous membrane material called Zeolitic Imidazolate Frameworks (ZIFs). ZIFs are synthesized through copolymerization of Zn(II) or Co(II) transition metals with imidazolate-type ($C_3N_2H_3^-$) linkers (Im)[2]. They are structurally similar to zeolites, where Si-O-Si bonds in zeolites are replaced by (Zn/Co)-Im-(Zn/Co) bonds in ZIFs in which case both bonds have ≈145° bond angles.

*Sorumlu yazar: ygurdal@atu.edu.tr
Geliş Tarihi: 15.02.2019, Kabul Tarihi: 01.07.2019

Although, zeolites are heavily used in industry for catalytic and membrane-based applications, one of their drawback appears in difficult incorporation of desired transition metals and organic linkers to their structures. ZIF structures, on the other hand, can be considered as a solution for overcoming the drawbacks in zeolite-based applications by improving performances through selectivity, electronic, and steric properties [3]. By changing transition metals and organic linkers in the structure, wide variety of ZIF membranes have been synthesized showing exceptional chemical and thermal stability and their electronic and structural properties have been tailored for a target application [4].

In terms of adsorption and membrane based separation of gas mixtures, ZIFs are mainly considered for separation of several gas mixtures, e.g., CO_2/CH_4, CO_2/CO, CO_2/H_2, CH_4/H_2, and CO_2/N_2 [5–9]. Although, their exceptionally high performance of gas separation and purification has been especially validated for CO_2 , CH_4 , and H_2 gas mixtures by many experimental and theoretical works [10,13], we know very little about potential of the ZIFs for separation of noble gas mixtures, such as Xe/Ar and Xe/Kr. Noble gases play significant role in both industry and biomedical applications including imaging, anesthesia, nuclear magnetic resonance, thanks to their chemical inertness, low solubility, and low conductivity. Noble gases and their radioisotopes are emitted to the atmosphere as a by product of nuclear fission [14]. Besides, during cryogenic distillation of air Xe/Kr mixture of 0.2/0.8 molar concentration is obtained where further distillation is required to obtain pure Xe and Kr. The current technologies for obtaining pure noble gases are energy intensive, hence, adsorption and diffusion based separation of noble gases using nanoporous materials should be encouraged for a cheaper and large scale purification of noble gases.

To date, there have been a few literature investigating noble gas separation performances of ZIFs. Wang et al. [15] both experimentally and theoretically investigate Xe adsorption capacity of ZIF-8, showing that at low pressures (< 1 bar) Xe uptake of ZIF-8 could reach 300 mg/g which is relatively a good performance comparing with other metal organic frameworks (MOFs), such as IRMOF-1 and UMCM-1. Same research group also show that Xe/Kr adsorption selectivity of CuBTC outperforms ZIF-8, by 6.7, which is attributed to the Xe uptake tendency of open metal sites present in CuBTC [12]. Magdysyuk et al. [16] investigate Xe and Kr adsorption in ZIF-8 and results show that while metal sites of ZIF-8 are not accessible by noble gases, imidazolate ligands shows tendecy for Xe and Kr adsorption. Gurdal and Keskin [17] computationally explore separation and purification of Xe/Ar and Xe/Kr gases in four ZIF structures, e.g, ZIF-1, ZIF-2, ZIF-3, and ZIF-10. According to the results, ZIF-1 and ZIF-2 shows higher Xe/Ar and Xe/Kr adsorption selectivities. Permeabilities of selected noble gas mixtures through ZIF membranes, on the other hand, follows the order of ZIF-2>ZIF-10>ZIF-3 and ZIF-10>ZIF-3>ZIF-2, respectively [18]. Literature on noble gas separation focuses on a few ZIF materials, hence, the noble gas separation performance analysis of several ZIFs is still lacking.

The scope of this work is to computationally explore adsorption and permeation selectivities of four representative ZIFs for Xe/Ar and Xe/Kr separations. We calculate single specie and binary adsorption of Xe, Ar, and Kr by varying pressures applying Grand Canonical Monte Carlo (GCMC) simulation method. Besides, self-diffusivities of Xe, Kr, as well as Ar species in their binary mixtures are calculated by classical molecular dynamics. We compare Xe/Kr and Xe/Ar uptakes, gas permeabilities, adsorption and permeation selectivities of ZIFs and discuss which material is more appropriate for noble gas separations and which property is playing a critical role in adsorption and membrane-based separation.

2. Computational Details

We use GCMC [19] simulation method to compute single specie adsorption of Xe, Kr, Ar and their binary mixture adsorptions in ZIFs. Gas diffusivities and permeabilities, on the other hand, are calculated using classical molecular dynamics simulations [20]. We focus on four representative ZIFs having Zn and Co metal atoms, linkers, prosities, and pore dimensions which are summarized in Table I. Among the ZIFs that we consider, ZIF-60 has the highest porosity, 70.82 %. While ZIF-6 and ZIF-60 have large pores, ZIF-65 and ZIF-79 have heterogeneity in pore sizes. All ZIFs contain Zn as transition metal center, except for ZIF-65 which has Co instead. In terms of organic linkers, all the ZIFs in this work have different organic linkers from each other. While ZIF-6 is (ZIF-65) composed of only Im (nIm) linkers, ZIF-60 (ZIF-79) possesses mixed organic linkers of Im and mIm (mbIm and nIm).

Tablo 1. Structural properties of ZIFs used in this work. For more details on structures, see Ref [19]. Imidazolate, methylimidazole, nitroimidazole, and methylbenzimidazole organic linkers in ZIFs are abbreviated as Im, mIm, nIm, and mbIm, respectively.

ZIF materials	Metal Atom	Linker	Porosity (%)	Pore size (Å)	Density (g/cm^3)	Volume (Å^3)
ZIF-6	Zn	Im	62.70	8.2/8.8	0.764	6940
ZIF-60	Zn	Im, mIm	70.82	7.2/9.4	0.769	14270
ZIF-65	Co	nIm	67.90	3.4/10.4	1.095	5152
ZIF-79	Zn	mbIm, nIm	56.87	4.0/7.5	1.075	11441

The atomic positions of all ZIFs under consideration are obtained from their XRD data [1-2]. Geometrical representations of ZIFs under consideration are depicted in Figure 1. Rigid structures of ZIFs are used throughout our simulations, which is shown to be an appropriate estimate in our previous works [17-18]. Spherical Lennard Jones 12-6 potentials are used to calculate atomic interactions [22]. Electrostatic interactions, on the the hand, are not considered which is shown to be an effective assumption for the calculations of Xe and Kr uptakes of several MOFs [23] . Lorentz-Berthelot mixing rules are applied to calculate gas-gas and gas-adsorbate cross interaction contribution. Force field parameters of the ZIF atoms are taken from Dreiding force field [24] and, if not available, Universal Force Field (UFF) [25] parameters are applied. Force field parameters of the gas species, instead, are taken from previous studies [17, 26]. The Xe/Kr gas update predictions of UFF and Dreeding force fields for several MOFs show good agreement with the experimental data [17]. A cutoff for the van der Waals interactions is set to 13 Å. While simulation box size of 2x2x2 is used for all GCMC simulations, it is increased up to 3x3x3 during the molecular dynamics runs. Periodic boundary conditions are always applied.

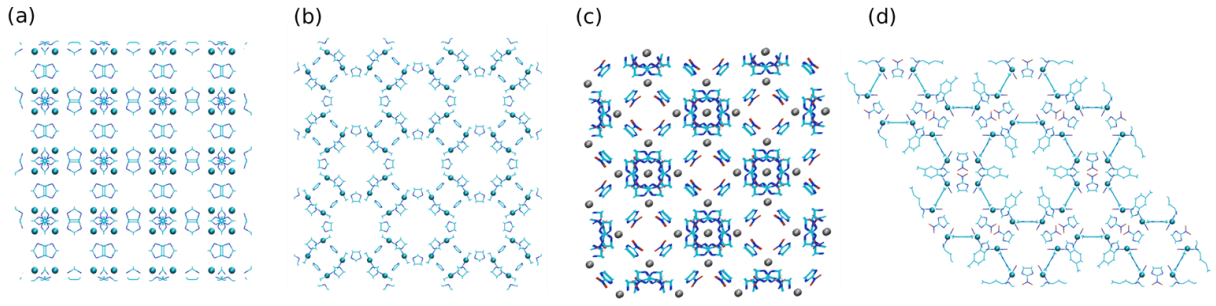

Figure 1. Ball and stick representations of a) ZIF-6, b) ZIF-60, c) ZIF-65, and d) ZIF-79. While organic linkers are depicted with sticks, metal atoms Zn and Co are shown with blue and grey balls, respectively.

Single component and mixture adsorption data of gases are calculated via conventional GCMC method. The temperature is set to 298 K, and pressure is increased from 1 bar to 10 bar, by 1 bar, and from 15 bar to 30 bar, by 5 bar. Using this temperature and pressure set-up, concentration of adsorbed phase molecules are determined at thermodynamic equilibrium. GCMC runs for each system at the lowest pressure are started from an empty ZIF structure. At higher pressures, on the other hand, the last configuration of the previous run is taken as a starting configuration of the next simulation. Simulations consists of $3x10^7$ trial configurations in total. While insertion, deletion, and translation moves are considered for single component adsorption calculations, a swap of gas particles are also considered for mixture adsorption runs. Adsorption selectivity of ZIFs for Xe from its binary mixtures are calculated using the standard definition below [27].

$$S_{ads}(i/j) = x_i/x_j \; y_i/y_j \tag{1}$$

where x and y are the adsorbed and feed gas phase molar fractions of the components in i/j mixture, respectively. We calculate mixture self-diffusivities of each components by classical molecular dynamics (MD) in NVT ensemble [28]. The self diffusivity, abbreviated as D_{self}, depicts the motion of

individual particles in a nanoporous material. D_{self} is calculated by Einstein relation as shown below [29],

$$D_{self} = \lim_{t\to\infty} \frac{1}{6t} \langle \frac{1}{N_t} \sum_{k=1}^{N_i} [r_{ik}(t) - r_{ik}(0)]^2 \rangle \quad (2)$$

where number of molecules is depicted by N and $r_{it}(t)$ shows the position of atom k of component i at time t. NVT ensemble average is denoted by angular brackets. Temperature is kept constant using the Nose-Hoover thermostat in all runs. We calculate D_{self} of each atomic types in Xe/Kr and Xe/Ar samples having 0.2/0.8 molar fractions at 10 bar. Initial MD states are created using appropriate loadings calculated by GCMC simulations. After equilibrating each system for about 8 ns with MD, production runs are collected for 16 ns. Permeation selectivities of ZIFs for Xe/Ar and Xe/Kr are calculated using following equation [18],

$$S_{permeation}(i/j) = \frac{x_i/x_j}{y_i/y_j} \frac{D_{self(i)}}{D_{self(j)}} \quad (3)$$

The equation above predicts a membrane's separation performance at a specific bulk pressure (10 bar in our case), and feed gas composition obtained by GCMC simulation (also at 10 bar) at room temperature. Gas permeability is another important criterion for deciding gas separation performances of nanoporous materials [30] which is calculated as:

$$P_i = \frac{c_i D_{self(i)} \vartheta}{f_i}$$

In the expression above, permeability of species i in mol/(msPa) is depicted by P_i, ϑ and c_i are the pore volume of the material and adsorbed concentration of species i in the mixture (mol/m^3), respectively. Feed gas fugacity of the species i, on the other hand, is depicted by f_i (Pa). Gas permeabilities of Xe is reported in Barrers in entire paper.

3. Results and Discussion

Single specie adsorption data of Xe, Ar, and Kr and their mixture adsorption data, Xe/Ar and Xe/Kr, in corresponding ZIFs at 298 K are depicted in Figure 2 as a function of bulk pressure. In generel, adsorption of single component Xe is larger than Kr and Ar in almost all ZIFs. The reason can be attributed to the energetic effects. As it can be seen from Figure 2, Xe atoms adsorb to ZIF pores and reaches saturation at lower pressures, however Kr and Ar atoms can still locate on adsorption sites in ZIF pores enabling them to reach saturation at higher pressures. Single component adsorption of Kr in ZIF-79 becomes slightly larger than Xe especially at higher pressures, entropic effects might be the reasoning. In ZIF-65 single component adsorption data of Xe and Kr are similar, especially at higher pressures. As it can be deduced from single component gas uptakes of ZIFs calculated by GCMC, mixture adsorption data show that ZIFs prefer Xe over Kr and Ar in both Xe/Kr and Xe/Ar samples. The reason is attributed to the strongly adsorbing Xe specie, which eliminates weakly adsorbing species of Kr and Ar in ZIFs. Xe uptake of ZIFs follows the order of ZIF-60> ZIF-79 > ZIF-6 > ZIF-65. While same ordering also applies for single component Kr adsorption, in the case of Ar uptake performances of ZIFs the ordering changes as ZIF-60 > ZIF-6 > ZIF-79 > ZIF-65. In the case of mixture adsorption simulations, we observe that, in general, adsorption amount of each specie decreases substantially. The difference between single component and mixture Xe uptake is significant in the case of Xe/Kr mixture adsorption with respect to Xe/Ar. For instance, while in ZIF-60 single component Xe uptake is 70 molecules/unitcell, in the case of mixture adsorption Xe adsorption decreases to 45 and 30 molecules/unitcell in Xe/Ar and Xe/Kr mixtures, respectively. The reason in attributed to the energetic effects. In mixture adsorption simulations Xe atoms has to compete with Kr and Ar adsorptions, where adsorption sites of ZIF structure are occupied by Kr and Ar atoms before

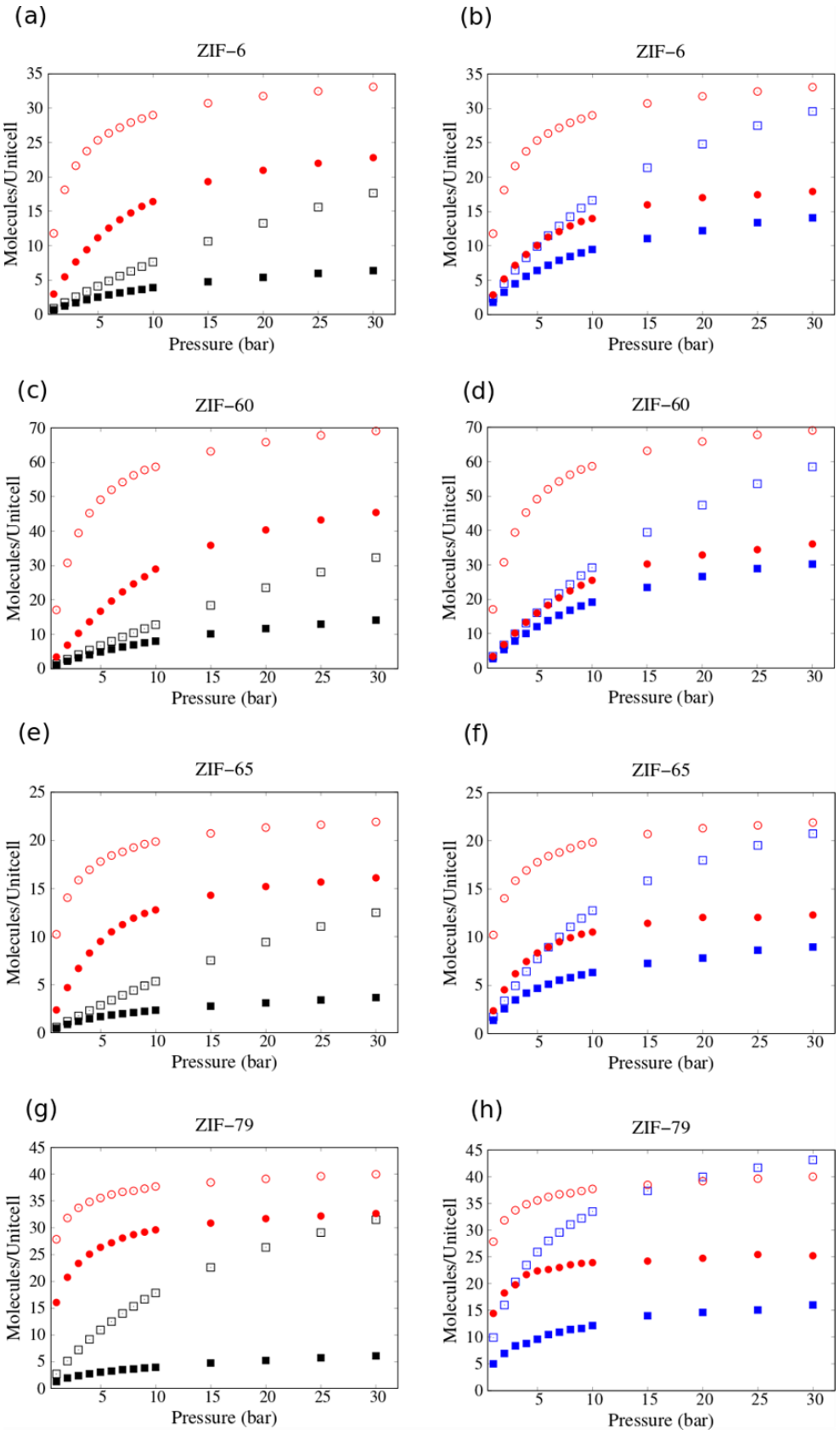

Figure 2. Single specie and mixture uptake data of Xe/Ar and Xe/Kr in (a - b) ZIF-6, (c - d) ZIF-60, (e - f) ZIF-65, and (g - h)ZIF-79. Gas uptake calculations are carried out at 298 K. The composition of feed gas is set to 0.2/0.8 for both Xe/Kr and Xe/Ar. While empty symbols show single component adsorption data of each species, filled symbols depict adsorption of species in binary mixtures. Black, red, and blue colors show the adsorption data of Ar, Xe, and Kr, respectively.

Xe adsorption, hence adsorption of Xe decreases in the mixture case. Comparing with Ar, Kr has larger energy parameter, hence, ZIF adsorption sites are more strongly occupied by Kr atoms explaining the larger decrease in Xe adsorption amount in Xe/Kr with respect to Xe/Ar. We also observe a decrease in Ar and Kr uptakes for gas mixtures with respect to their single component adsorption data. For Ar, this result is more pronounced in the case of ZIF-79 where at 30 bar single component Ar adsorption of 30 molecules/unitcell decreases to 3 molecules/unitcell in Xe/Ar mixture adsorption. In the case of Kr, 43 molecules/unitcell single adsorption amount in ZIF-79 falls to 10 molecules/unitcell in Xe/Kr mixture adsorption.

Mixture adsorption GCMC data is used to calculate Xe adsorption selectivities of ZIFs and predict their adsorption-based noble gas separation performances. For an adsorption-based gas mixture separations, sustaining the selectivity across several pressure ranges is one of the most important characteristics of promising adsorbents. The adsorption selectivities of Xe/Ar and Xe/Kr mixtures having 0.2/0.8 molar fractions are shown in Figure 3 as a function of pressure. Selectivity values larger than 1 indicates that ZIFs are selectively separate Xe from its mixtures of Xe/Kr and Xe/Ar. ZIF-79 shows the largest Xe adsorption selectivity for both Xe/Ar and Xe/Kr. The trend in Xe adsorption selectivity of all ZIFs, especially the ordering of ZIF-79 > ZIF-65 > ZIF-6 > ZIF-60, is similar for both Xe/Kr and Xe/Ar samples. ZIF-79 shows larger Xe adsorption selectivity especially at low pressures, between 1 bar and 10 bar. The other ZIFs, instead, show slight decrease in Xe adsorption selectivity with increase in pressure. All the ZIFs that we consider, Xe adsorption selectivity decreases gradually as pressure increases. This effects is more pronounced in ZIF-79, where Xe adsorption selectivity of 50 (12) in Xe/Ar (Xe/Kr) mixture at 1 bar, drops to 20 (7) at 30 bar.

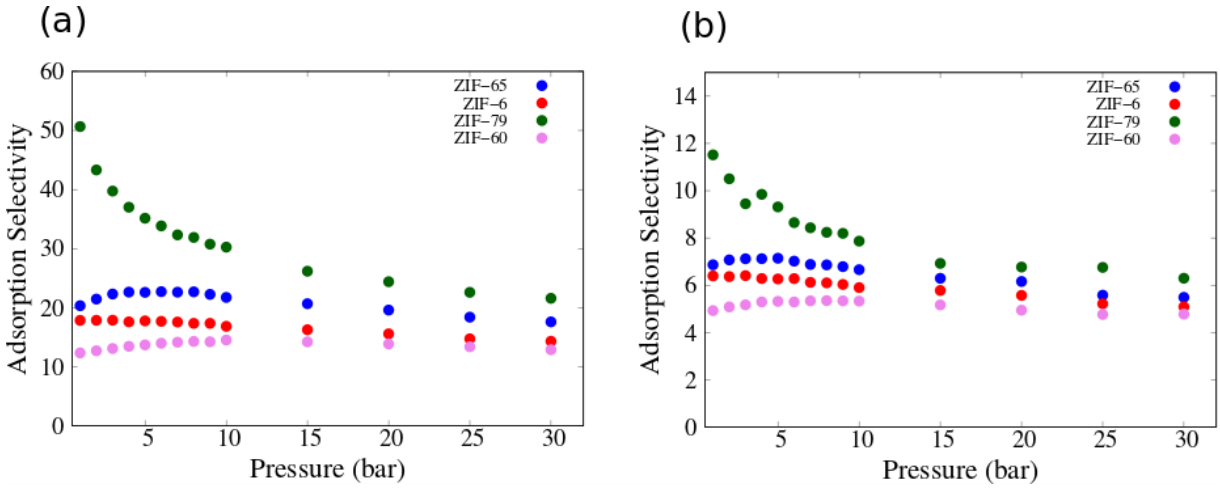

Figure 3. Adsorption selectivity of ZIFs with respect to feed pressure for (a)Xe/Ar and (b)XeKr separations.

Concerning the pore dimensions of the ZIFs under consideration, ZIF-79 and ZIF-65 have heterogeneous pore dimensions being 4.0/7.5 Å and 3.4/10.4 Å respectively, see Table 1. ZIF-60 and ZIF-6, on the other hand, have larger pore dimensions. Our results show that ZIFs possessing heterogenous pore sizes favor more Xe adsorption which leads to larger Xe adsorption selectivities. Larger pore sizes, instead, enables adsorption of each species which results in lower Xe uptake selectivities for both Xe/Kr and Xe/Ar samples. Entropic effects are considered to be the main reason of this observation. Xe atom shows strong confinement with the ZIFs having smaller pores. The confinement of Kr and Ar, on the other hand, can be thought as being smaller and being similar in both small and larger pores leading to comparable adsorption strength. The enchanced confinement of Xe in ZIFs having small pores, thus, results in larger Xe adsorption selectivities. Our result also agrees with the literature where MOFs having heterogeneous pore-sizes, such as ZIF-1 and ZIF-2, also show larger Xe adsorption selectivities with respect to the MOFs with larger pores [17]. One another important observation from Figure 3 is that, Xe adsorption selectivity from Xe/Ar are always larger than the selectivity observed for Xe/Kr. As it is expected, adsorption selectivity of Xe enhances when it is mixed

with an atom having smaller energy parameter, Ar, with respect to the atoms having larger energy parameters, Kr.

For determining overall noble gas separation performances of ZIFs under consideration, the transport rates of gas species should be also considered. We compute self diffusivities of gas species using MD, and calculate Xe permeabilities and permeation selectivities in Xe/Ar and Xe/Kr mixtures with 0.2/0.8 gas composition at 10 bar and 298 K. The results are summarized in Table 2. As a general observation, Xe diffuses slower than Kr and Ar components due to its stronger adsorption on ZIF pores. For instance, in ZIF-6, Xe and Ar (Kr) self-diffusivities in Xe/Ar (Xe/Kr) mixture are calculated as $5x10^{-5}$ ($4.37x10^{-5}$) cm^2/s and $2.57x10^{-4}$ ($1x10^{-4}$) cm^2/s, respectively. In the case of ZIF-79, on the other hand, Xe and Ar (Kr) self-diffusivities in Xe/Ar (Xe/Kr) mixture is computed as $1.77x10^{-6}$ ($2.38x10^{-6}$) cm^2/s and $1.20x10^{-5}$ ($8.16x10^{-6}$) cm^2/s, respectively. We notice that, although ZIF-79 shows promising character as an adsorbent by separating Xe from both Xe/Kr and Xe/Ar, Xe diffusion in ZIF-79 pores is limited due to stronger interaction of Xe with ZIF-79 adsorption sites, as well as smaller pore distribution of ZIF-79. Comparing Kr and Ar separations, Kr adsorbs stronger than Ar in ZIF pores which leads to slower diffusion of Kr with respect to Ar in binary diffusion simulations.

We predict Xe permeabilities and permeation selectivities of ZIFs for dual mixtures of Xe, Kr, and Ar, see Table 2. A promising nanoporous material for a permeation-based separation of a specific gas from its mixture should possess high permeation selectivity as well as high permeability. High permeability is an important criterion for industrial-scale gas separations, since it succeeds higher gas purification with smaller membrane area, hence lowering capital cost. Xe permeation selectivities of ZIFs become significantly smaller with respect to their Xe adsorption selectivities. The reason is attributed to the enchanced confinement of Xe atom in ZIF pores which leads to its slower diffusion and compensates its larger adsorption selectivity. For Xe/Ar mixture, ZIF-6 shows the largest Xe permeability with respect to the other ZIFs due to its homogeneously distributed large pores. Considering permeation selectivities, on the other hand, ZIF-6 shows the poorest performance since larger pores also allow Ar diffusion leading to smaller Xe permeation selectivity. For Xe/Kr mixture, on the other hand, while ZIF-60 has the highest Xe permeation selectivity, the highest Xe permeability is observed in ZIF-6. Taking the results into consideration, ZIF-60 showing high Xe permeation selectivity and also high Xe permeability can be considered as a promising candidate for membrane-based separation of Xe from its binary mixtures.

Tablo 2. Mixture self-diffusivities of Xe ($D_{self\,(Xe)}$), Xe permeation selectivities ($S_{permeation}$), Xe permeabilities in ZIFs for both Xe/Ar and Xe/Kr mixtures are reported.

ZIF materials	$D_{self\,(Xe)}$ in Xe/Ar (cm^2/s)	$D_{self\,(Xe)}$ in Xe/Kr (cm^2/s)	$S_{permeation}$ (Xe/Ar)	$S_{permeation}$ (Xe/Kr)	P_{Xe} in Xe/Ar ($/10^2$ Barrer)	P_{Xe} in Xe/Kr ($/10^2$ Barrer)
ZIF-6	$5.02x10^{-5}$	$4.37x10^{-5}$	3.28	2.56	1847.34	1369.82
ZIF-60	$3.71x10^{-5}$	$4.06x10^{-5}$	3.52	2.82	1323.78	1275.27
ZIF-79	$1.77x10^{-6}$	$2.38x10^{-6}$	4.47	2.28	61.30	66.46

We observe single-file diffusion of Xe for both Xe/Kr and Xe/Ar samples in ZIF-65. The self-diffusivities of gas particles can be considered as normal when gas molecules can pass one another in the pores of nanoporous materials. The reverse situation, on the other hand, is considered as single file diffusion when gas molecules of one specie cannot pass one another in the pore leading to only small fluctuations in the mean-square displacement of the particle in three dimensions over simulation time [31]. ZIF-65 has heterogeneous pores with the size of 3.4/10.4 Å where steric hindrance and topology effects become dominant for Xe preventing its diffusion from the pores. Single file diffusion of Xe is also observed in zeolite AlPO4-31 by molecular dynamics study of Sholl et al. [32]. Since we do not observe diffusion of Xe, Xe permeability and permeation selectivity values are not calculated for ZIF-65.

4. Conclusions

We investigate adsorption and diffusion-based noble gas separation performances of ZIF membranes, particularly ZIF-6, ZIF-60, ZIF-65, and ZIF-79 using GCMC and MD simulations. Results show that

ZIF-79 has the highest Xe uptake selectivities for both Xe/Kr and Xe/Ar mixtures. ZIF-79 has heterogeneous and small pore distribution which potentially creates stronger confinement for Xe atom, thus, explaining higher uptake of Xe over the other ZIFs. ZIFs showing a good performance for adsorption-based Xe separation, are shown to be poor for Xe permeation. While ZIF-79 can be a promising candidate for adsorption-based purification of Xe, however Xe diffusion is limited in ZIF-79 which can be the side effects of stronger adsorbate-adsorbent interactions as well as steric hindrance effects observed in ZIF-79. We suggest that ZIFs possessing heterogeneous and relatively small pore distribution are ideal candidates for adsorption-based separation of Xe. Concerning gas permeabilities, ZIF-6 shows the highest Xe permeabilities for both Xe/Kr and Xe/Ar mixtures, which is related with its homogeneously distributed large pores. However, its larger pores also allow Kr and Ar diffusion, thus, reducing Xe permeation selectivity of ZIF-6. ZIF-60, on the other hand, showing both high Xe permeation selectivity and Xe permeability can be a potential candidate for diffusion-based separation of Xe. Our results suggest that ZIFs that are promising candidates for adsorption-based separation of noble gases might not satisfy also membrane-based separation at the same time. Nonetheless, ZIFs that are investigated in this study are shown to be better adsorbents and membranes than zeolites [33] and polymeric membranes [34].

Acknowledgement

The numerical calculations reported in this paper were fully performed at TUBITAK ULAKBIM, High Performance and Grid Computing Center (TRUBA resources), located in Turkey.

References

[1] Park K.S., Ni Z., Cote A.P., Choi J.Y., Huang R., Uribe-Romo F.J., Chae H.K., O'Keeffe M., Yaghi O. M. 2006. Exceptional Chemical and Thermal Stability of Zeolitic Imidazolate Frameworks. Proceedings of the National Academy of Sciences, 103 (27): 10186–10191.

[2] Banerjee R., Phan A., Wang B., Knobler C., Furukawa H., O'Keeffe M., Yaghi O.M. 2008. High-throughput Synthesis of Zeolitic Imidazolate Frameworks and Application to CO_2 Capture. Science, 319 (5865): 939–943.

[3] Grau-Crespo R., Aziz A., Collins A.W., Crespo-Otero R., Hernández N.C., Rodriguez Albelo L.M., Ruiz-Salvador A.R., Calero S., Hamad S. 2016. Modelling a Linker Mix and Match Approach for Controlling the Optical Excitation Gaps and Band Alignment of Zeolitic Imidazolate Frameworks. Angewandte Chemie International Edition, 55 (52): 16012–16016.

[4] Banerjee R., Furukawa H., Britt D., Knobler C., O'Keeffe M., Yaghi O.M. 2009. Control of Pore Size and Functionality in Isoreticular Zeolitic Imidazolate Frameworks and Their Carbon dioxide Selective Capture Properties. Journal of the American Chemical Society, 131 (11): 3875–3877.

[5] Liu J., Keskin S., Sholl D.S., Johnson J.K. 2011. Molecular Simulations and Theoretical Predictions for Adsorption and Diffusion of CH_4/H_2 and CO_2/CH_4 Mixtures in Zifs. The Journal of Physical Chemistry C, 115 (25): 12560–12566.

[6] Liu Y., Hu E., Khan E.A., Lai Z. 2010. Synthesis and Characterization of Zif-69 Membranes and Separation for CO_2/CO Mixture. Journal of Membrane Science, 353 (1): 36–40.

[7] Yumru A.B., Safak Boroglu M., Boz I. 2018. Zif-11/matrimid R Mixed Matrix Membranes for Efficient CO_2, CH_4, and H_2 Separations. Greenhouse Gases: Science and Technology, 8 (3): 529–541.

[8] Battisti A., Taioli S., Garberoglio G. 2011. Zeolitic Imidazolate Frameworks for Separation of Binary Mixtures of CO_2, CH_4, N_2 and H_2: A Computer Simulation Investigation. Microporous and Mesoporous Materials, 143 (1): 46–53.

[9] Chokbunpiam T., Fritzsche S., Chmelik C., Caro J., Janke W., Hannongbua S. 2016. Gate Opening, Diffusion, and Adsorption of CO_2 and N_2 Mixtures in Zif-8, The Journal of Physical Chemistry C, 120 (41): 23458–23468.

[10] McDaniel J.G., Yu K., Schmidt J.R. 2012. Ab Initio, Physically Motivated Force Fields for CO_2 Adsorption in Zeolitic Imidazolate Frameworks. The Journal of Physical Chemistry C, 116 (2): 1892–1903.

[11] Chen B., Yang Z., Zhu Y., Xia Y. 2014. Zeolitic Imidazolate Framework Materials: Recent Progress in Synthesis and Applications. Journal of Material Chemistry A, 2: 16811–6831.
[12] Günay Sezer G., Erucar I. 2017. Hydrothermal Synthesis, Crystal Structure, and Properties of 1D Zigzag Chain Zinc(ii) Coordination Polymer Constructed From Nicotinic Acid and 1,4-bis(imidazol-1-ylmethyl) benzene. Journal of the Turkish Chemical Society, Section A: Chemistry, 23–38.
[13] Gulcay, E., Erucar, I. 2019. Molecular Simulations of Cofs, Irmofs and Zifs for Adsorption-based Separation of Carbon Tetrachloride from Air. Journal of Molecular Graphics and Modelling, 86: 84–94.
[14] Wang Q., Xiong S., Xiang Z., Peng S., Wang X., Cao D. 2016. Dynamic Separation of Xe and Kr by Metal-Organic Framework and Covalent-Organic Materials: A Comparison with Activated Charcoal. Science China Chemistry, 59 (5): 643–650.
[15] Wang Q., Wang H., Peng S., Peng X., Cao D. 2014. Adsorption and Separation of Xe in Metal–Organic Frameworks and Covalent–Organic Materials. The Journal of Physical Chemistry C, 118 (19): 10221–10229.
[16] Magdysyuk O.V., Adams F., Liermann H.-P., Spanopoulos I., Trikalitis P.N., Hirscher M., Morris R.E., Duncan M.J., McCormick L.J., Dinnebier R.E. 2014. Understanding the Adsorption Mechanism of Noble Gases Kr and Xe in CPO-27-Ni, CPO-27-Mg, and Zif-8. Physical Chemistry Chemical Physics, 16: 23908–23914.
[17] Gurdal Y., Keskin S. 2012. Atomically Detailed Modeling of Metal Organic Frameworks for Adsorption, Diffusion, and Separation of Noble Gas Mixtures. Industrial & Engineering Chemistry Research, 51 (21): 7373–7382.
[18] Gurdal Y., Keskin S. 2013. Predicting Noble Gas Separation Performance of Metal Organic Frameworks Using Theoretical Correlations. The Journal of Physical Chemistry C, 117 (10): 5229–5241.
[19] Allen M., Tildesley J. 1987. Computer Simulations of Liquids. Oxford Science Publications, Oxford.
[20] Frenkel D., Smit B. 1987. Understanding Molecular Simulation: From Algorithms to Applications. Academic Press, San Diego.
[21] Atci E., Keskin S. 2012. Understanding the Potential of Zeolite Imidazolate Framework Membranes in Gas Separations Using Atomically Detailed Calculations. The Journal of Physical Chemistry C, 116 (29): 15525–15537.
[22] Maitland G.C., Rigby M., Smith E.B., Wakeham W.A. 1981. Intermolecular Forces: Their Origin and Determination. Clarendon Press, Oxford.
[23] Ryan P., Farha O.K., Broadbelt L.J., Snurr R.Q. 2011. Computational Screening of Metal-Organic Frameworks for Xenon/Krypton Separation, AIChE Journal, 57 (7): 1759–1766.
[24] Mayo S L., Olafson B.D., Goddard W.A. 1990. Dreiding: A Generic Force Field for Molecular Simulations. The Journal of Physical Chemistry, 94 (26): 8897–8909.
[25] Rappe A.K., Casewit C.J., Colwell K.S., Goddard W.A., Skiff W M. 1992. UFF, A full Periodic Table Force Field for Molecular Mechanics and Molecular Dynamics Simulations. Journal of the American Chemical Society, 114 (25): 10024–10035.
[26] Talu O., Myers A.L. 2001. Reference Potentials for Adsorption of Helium, Argon, Methane, and Krypton in High-Silica Zeolites. Colloids and Surfaces A: Physicochemical and Engineering Aspects, 187-188, 83–93.
[27] Gurdal Y., Keskin S. 2016. A New Approach for Predicting Gas Separation Performances of Mof Membranes, Journal of Membrane Science, 519: 45–54.
[28] Ackerman D.M., Skoulidas A.I., Sholl D.S., Johnson J.K. 2003. Diffusivities of Ar and Ne in Carbon Nanotubes. Molecular Simulation, 29 (10-11): 677–684.
[29] Keil F., Krishna R., Coppens M. 2011. Modeling of Diffusion in Zeolites. Reviews in Chemical Engineering, 16: 71–197.
[30] Altintas C., Keskin S. 2017. Molecular Simulations of Mof Membranes for Separation of Ethane/Ethene and Ethane/Methane Mixtures. RSC Advances, 7: 52283–52295.
[31] Keffer D., McCormick A., Davis H. 1996. Unidirectional and Single-file Diffusion in AlPO4-5: Molecular Dynamics Investigations. Molecular Physics, 87 (2): 367–387.

[32] Sholl D.S., Lee C.K. 2000. Influences of Concerted Cluster Diffusion on Single-file Diffusion of CF4 in Alpo4-5 and Xe in Alpo4-31. The Journal of Chemical Physics, 112 (2): 817–824.
[33] Sumer Z., Keskin S. 2017. Molecular Simulations of Mof Adsorbents and Membranes for Noble Gas Separations. Chemical Engineering Science, 164: 108–121.
[34] Nakai Y., Yoshimizu H., Tsujita Y. 2005. Enhanced Gas Permeability of Cellulose Acetate Membranes Under Microwave Irradiation. Journal of Membrane Science, 256 (1): 72–77.